Available online at www.sciencedirect.com
SCIENCE DIRECT®
Journal of the European Ceramic Society 25 (2005) 1033–1039
www.elsevier.com/locate/jeurceramsoc

Hot corrosion behavior of Ti_3SiC_2 in the mixture of Na_2SO_4–NaCl melts

Guangming Liu [a,b,*], Meishuan Li [a], Yanchun Zhou [a], Yaming Zhang [a]

[a] *Shenyang National Laboratory for Materials Science, Institute of Metal Research, Chinese Academy of Sciences, Shenyang 110016, China*
[b] *Department of Materials Science and Engineering, Nanchang Institute of Aeronautical Technology, Nanchang 330034, China*

Received 30 November 2003; received in revised form 7 April 2004; accepted 16 April 2004
Available online 10 July 2004

Abstract

The corrosion behavior of polycrystalline Ti_3SiC_2 was studied in the mixture of Na_2SO_4–NaCl melts with various mass ratios at 850 °C. The results demonstrated that Ti_3SiC_2 suffered from serious hot corrosion attack in the mixture of Na_2SO_4–NaCl melts when the concentration of Na_2SO_4 was higher than 35 wt.%. A large amount of corrosion products spalled from specimens during the tests and obvious mass loss was observed. Hot corrosion of Ti_3SiC_2 would become severe because NaCl had lower melting-point and caused Na_2SO_4–NaCl mixture melted below 850 °C. However, when the concentration of Na_2SO_4 was lower than 25 wt.% in the mixture, a protective oxide layer ($SiO_2 + TiO_2$) formed on the substrate, the corrosion rate of Ti_3SiC_2 became quite slow and slight mass gain was observed, the corrosion products did not spall from substrate at 850 °C. The microstructure and phase composition of the corroded samples were investigated by SEM/EDS and XRD.

Keywords: Ti_3SiC_2; Corrosion; Molten salts; Hot corrosion; Na_2SO_4–NaCl melts

1. Introduction

Ceramics are generally thought to possess many of the properties desired for higher-temperature replacements of superalloy: high melting points, high-temperature strength, low density, and increased resistance to aggressive environments. The primary shortcoming of monolithic ceramics is their lack of acceptable low-temperature ductility and toughness. Ti_3SiC_2 with a layered crystal structure possesses a combination of the properties of both metals and ceramics. The theoretical density is 4.53 g cm^{-3}.[1] It has a hardness of 4 GPa, a Young's modulus of 325 GPa, a room temperature fracture toughness about 7 MPa m$^{1/2}$ and quite damage tolerant. It exhibits a brittle-to-plastic transition around 1100 °C; at 1300 °C, the material is plastic with 'yield' point of 100 and 500 MPa in flexure and compression, respectively. At room temperature, it has electrical and thermal conductivities of $4.5 \times 10^6\ \Omega^{-1}\,m^{-1}$ and 37 W m^{-1} K^{-1}, respectively.[1–6] These unusual combinations of the properties render it a candidate structural material for high-temperature applications. When it was oxidized in air, a protective oxide scale formed in layers, where the inner layer was composed of a mixture of SiO_2 and TiO_2 and the outer layer was pure TiO_2. Oxidation kinetics follows a parabolic law in the 900–1300 °C temperature range with an activation energy of about 370 kJ mol^{-1}.[7]

Industry systems are such as heat engines and heat exchangers involve harsh environments. The structural materials are subjected to high temperatures, corrosive gases and condensed phases such as NaCl and Na_2SO_4. Under the appropriate conditions these salts deposit on substrate, which lead to severe hot corrosion attack and accelerated degradation of materials.[8] From the point of view of application, to evaluate corrosion resistance of a material is important in corrosive environments. Liu et al.[9–11] studied the hot corrosion behavior of polycrystalline Ti_3SiC_2 induced by molten Na_2SO_4 and Li_2CO_3–K_2CO_3, respectively. The results demonstrated that Ti_3SiC_2 ceramics coated with about 2 mg cm^{-2} Na_2SO_4 suffered from serious hot corrosion at 900 and 1000 °C.[11] When Ti_3SiC_2 was immersed in K_2CO_3–Li_2CO_3 eutectic mixture in the 700–850 °C temperature range, obvious mass loss was ob-

* Corresponding author. Tel.: +86 791 8211519; fax: +86 791 8224727.
E-mail addresses: gmliu@imr.ac.cn, gmliu@niat.jx.cn (G. Liu).

0955-2219/$ – see front matter © 2004 Elsevier Ltd. All rights reserved.
doi:10.1016/j.jeurceramsoc.2004.04.013

served, severe hot corrosion occurred and led to strength degradation.[9,10] However, up to now, investigations focused on the corrosion behaviors of Ti_3SiC_2 in the mixed salts of Na_2SO_4 + NaCl were seldom reported. The aim of this work is to report the hot corrosion behaviors of Ti_3SiC_2 in the mixture of Na_2SO_4–NaCl melts. The results are useful for selecting the appropriate conditions for the application of this technologically important material.

2. Experimental

2.1. Specimen preparation

Ti_3SiC_2 used in this work was TSC^{ZS510}, which was fabricated by the in situ hot pressing/solid–liquid reaction process, which was described elsewhere.[12] The Ti_3SiC_2 content was determined to be 93 wt.% by the Rietveld method in Cerius[2] computational program for material research (MSI, USA) using DBWS code and the major impurity was TiC. The density of the materials is 4.52 gcm^3, and the porosity is less than 1%. Rectangular specimens with dimensions of 8 mm × 8 mm × 2.5 mm were cut by the electrical-discharge method. The surfaces were polished down to 800-alumina paper. The specimens were cleaned in acetone, ethanol, and distilled water in an ultrasonic bath before tests.

2.2. Specimen examination

The mixed Na_2SO_4–NaCl powders were prepared according to the Na_2SO_4:NaCl mass ratios of 0.75:0.25, 0.35:0.65, and 0.25:0.75, respectively. In each test, one sample and mixed Na_2SO_4–NaCl salts were put into an Al_2O_3 crucible, and then it was placed in an electric box furnace. The tests were conducted at 850 °C in air. The specimens were immersed in the molten salts completely during the tests. In order to probe the influence of NaCl in the mixed salts, the corrosion behavior of Ti_3SiC_2 in pure molten NaCl was also conducted at 850 °C.

After hot corrosion tests, the samples were washed with boiling distilled water to dissolve the remains of Na_2SO_4–NaCl and other dissolvable salts, then the samples were dried in hot air. Each sample was weighted before and after the test (the sensitivity of the balance used was 10^{-5} g). The microstructure analysis of corroded specimens was carried out by using a scanning electron microscope (SEM) equipped with an energy dispersive spectroscope (EDS). The phase compositions of the corrosion layer were determined by X-ray diffraction (XRD).

3. Results and discussion

3.1. Kinetics of hot corrosion

Fig. 1 shows the mass change per unit area of Ti_3SiC_2 as a function of time during the hot corrosion in the mixture of Na_2SO_4–NaCl melts and pure molten NaCl at 850 °C. When specimen corroded in 75 wt.% Na_2SO_4 + 25 wt.% NaCl mixture for 8 h, the mass change per unit area (ΔW) decreased monotonically. The final mass loss was about 70 mg cm^{-2} after 8 h. The results revealed that severe hot corrosion occurred during the test. When the specimen corroded in the mixture of 35 wt.% Na_2SO_4 + 65 wt.% NaCl melts, although the mass loss and mass gain occurred alternately, the mass loss per unit area was observed as a whole. The final mass loss was about 70 mg cm^{-2}.

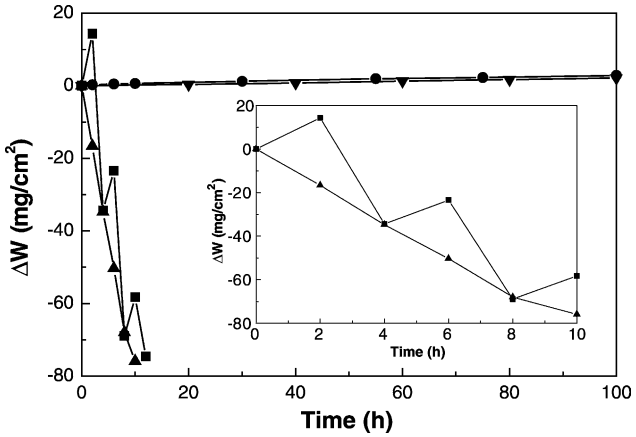

Fig. 1. The mass change per unit area as a function of time for hot corrosion of Ti_3SiC_2 in the mixture of Na_2SO_4–NaCl and NaCl melts at 850 °C. (▲) 75 wt.% Na_2SO_4 + 25 wt.% NaCl; (■) 35 wt.% Na_2SO_4 + 65 wt.% NaCl; (●) 25 wt.% Na_2SO_4 + 75 wt.% NaCl; (▼) NaCl.

On contrary to above mentioned, obvious mass loss, it is surprising that monotonous and slight mass gain (about 2 mg cm^{-2}) was observed when the specimens corroded in both mixture of 25 wt.% Na_2SO_4 + 75 wt.% NaCl melts and pure NaCl melt even for 100 h. It suggested that the corrosion products did not spall from specimens on a large scale during the hot corrosion. Therefore, it could be concluded at this point that Ti_3SiC_2 suffered disastrous hot corrosion in the mixture of Na_2SO_4 + NaCl melts when the concentration of Na_2SO_4 was higher than 35 wt.%.

3.2. Phase composition and microstructure of the corrosion products

Fig. 2a shows the surface morphology of Ti_3SiC_2 after hot corrosion in the mixture of 75 wt.% Na_2SO_4–25 wt.% NaCl melts for 8 h at 850 °C. The corrosion products spalled off on a large scale from the sample surface. Therefore, the surface morphology was differentiated into two typical regions: P is the bottom surface from which the corrosion products spalled off, T is the original surface of the outer corrosion scale, where the corrosion products did not spall off. Fig. 2b and c show higher magnification of region T and P, respectively. The corresponding EDS X-ray spectra were also included in both figures. In order to probe the phase compositions of two different regions, the outer layer corro-

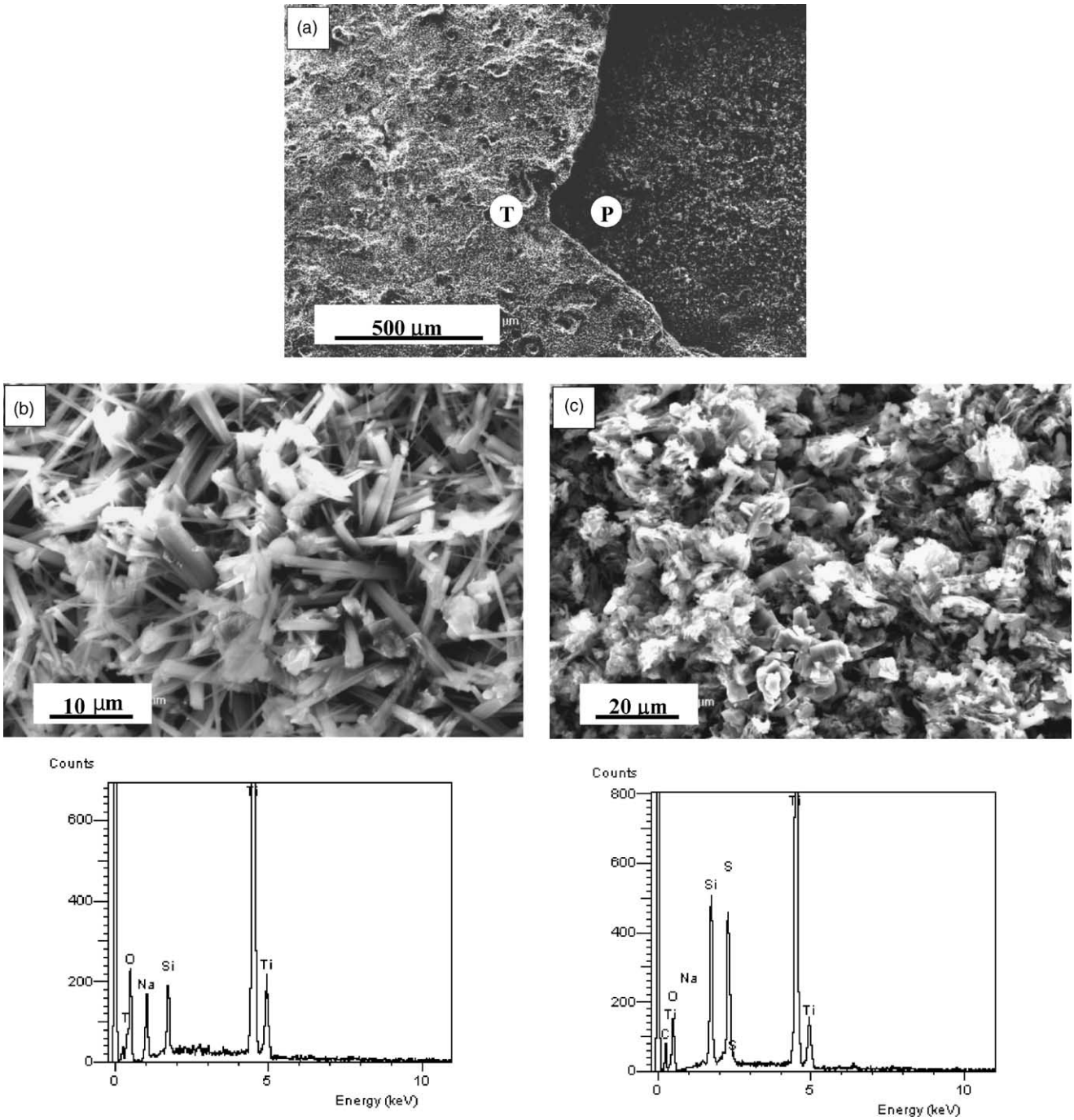

Fig. 2. The surface morphologies and corresponding EDS X-ray spectra of Ti_3SiC_2 after hot corrosion in the mixture of 75 wt.% Na_2SO_4–25 wt.% NaCl melts for 8 h at 850 °C. (a) Overview; (b) higher magnification of region T; (c) higher magnification of region P.

sion products were peeled off completely, and collected, and then the phase compositions of two regions (region T and region P) could be identified by XRD. Fig. 3 shows XRD patterns of the region T and P. It is seen from Fig. 2b that the surface of the region T consists of a number of a circular crystallites. EDS analysis demonstrated that the elements in this region were consisted of Ti, O, Si, and Na. Combining the results of XRD and EDS, the main phases in this region were recognized as $Na_{0.23}TiO_2$, $Na_2Ti_6O_{13}$, TiO_2 and a small amount of Na_2SiO_3. In Fig. 2c, irregular protrusions formed in region P, which morphology is different from the region T. In region P, TiO_2 and sulfur were identified as the main phases by XRD and EDS.

Fig. 4a and b are cross-sections of the sample corroded in the mixture of 75 wt.% Na_2SO_4 + 25 wt.% NaCl melts. SEM observation revealed that the cross-sections had a two-layer microstructure. Many micro-pores were observed in the outer layer. Some radial and transverse cracks ex-

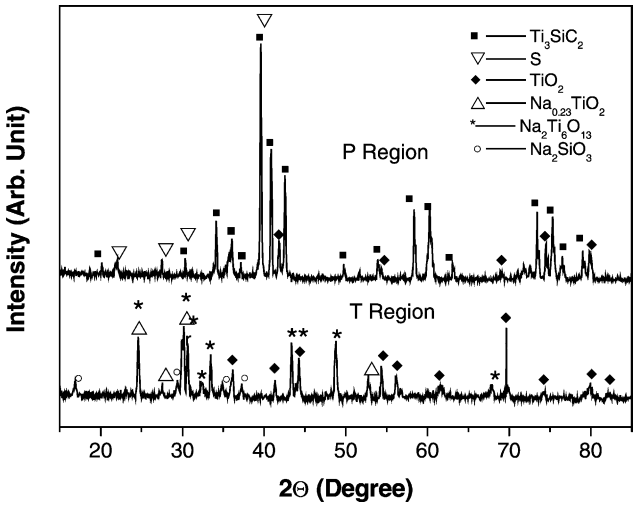

Fig. 3. XRD patterns of region P and region T.

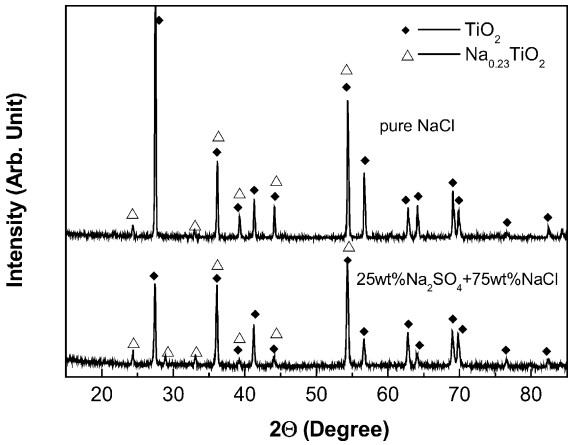

Fig. 5. XRD patterns of specimens corroded in the mixture of 25 wt.% Na_2SO_4–75 wt.% NaCl melts and NaCl melt at 850 °C for 100 h.

isted in the outer and inner layer, respectively. Because two types of crack co-existed in the outer and inner corrosion layer, furthermore, sulfur segregated in the inner layer and resulted in weak bonding between the inner layer and outer layer, the outer layer spalled off easily during hot corrosion and subsequent treatments. The other mechanism for the spallation of corrosion products from substrate might be related to the Na^+ presented in the mixed molten salts. It is reported that Na^+ could induce devitrification in amorphous SiO_2.[13] The resultant volume change could lead to cracking and a breakdown of the protective SiO_2 layer. Thus, even acidic salts might lead to degradation of SiO_2-protected ceramics via this mechanism. Because corrosion products spalled from specimens on a large scale, protective corrosion products could not form on the substrate, severe hot corrosion would sustain.

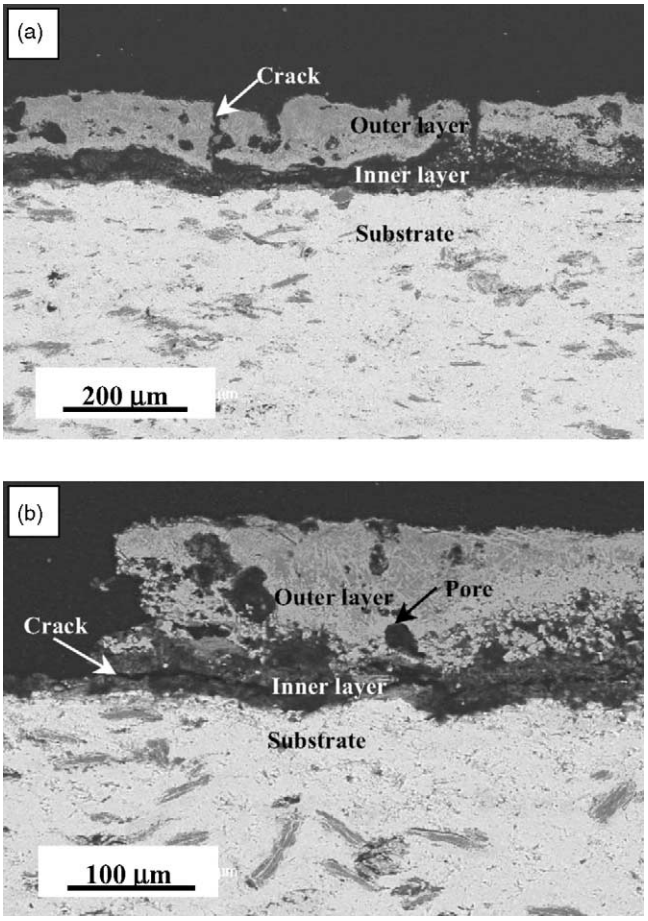

Fig. 4. The cross-sections of specimen corroded in the mixture of 75 wt.% Na_2SO_4–25 wt.% NaCl melts at 850 °C for 8 h. (a) Overview; (b) higher magnification.

Fig. 5 shows the X-ray diffraction patterns of the corroded sample in the mixture of 25 wt.% Na_2SO_4 + 75 wt.% NaCl melts. The main phases of corrosion products were identified as TiO_2 and $Na_{0.23}TiO_2$. Fig. 6a and b are surface morphology and cross-section of specimen corroded in the mixture of 25 wt.% Na_2SO_4 + 75 wt.% NaCl melts, respectively. Although in Fig. 6a some cracks were observed on the surface of corrosion layer, corrosion products did not spall from the specimen. The large grains on the surface were recognized as TiO_2, and the small grains were $Na_{0.23}TiO_2$ by EDS. The cross-section of corroded samples had a duplex microstructure, i.e. an outer layer and an inner layer (divided by white mark line). In outer layer the light gray grains were recognized as TiO_2, the dark gray grains were identified as $Na_{0.23}TiO_2$. EDS analysis revealed that the main phases in the inner layer were TiO_2 and SiO_2. The reason for the fact that no crystalline Si-containing phase was detected by XRD might be related to the following reasons. One possible reason was due to relative content of SiO_2 in the corrosion products was too low to be detected. The other reason was related to the thickness of the outer layer (about 15 μm), which led to characteristic peaks of Si-containing phase in the inner layer could not be detected by XRD. Similarly, in Fig. 6b some pores were observed in the cross-section.

Fig. 7a and b are surface morphology and cross-section of the specimen corroded in the pure NaCl melt, respectively.

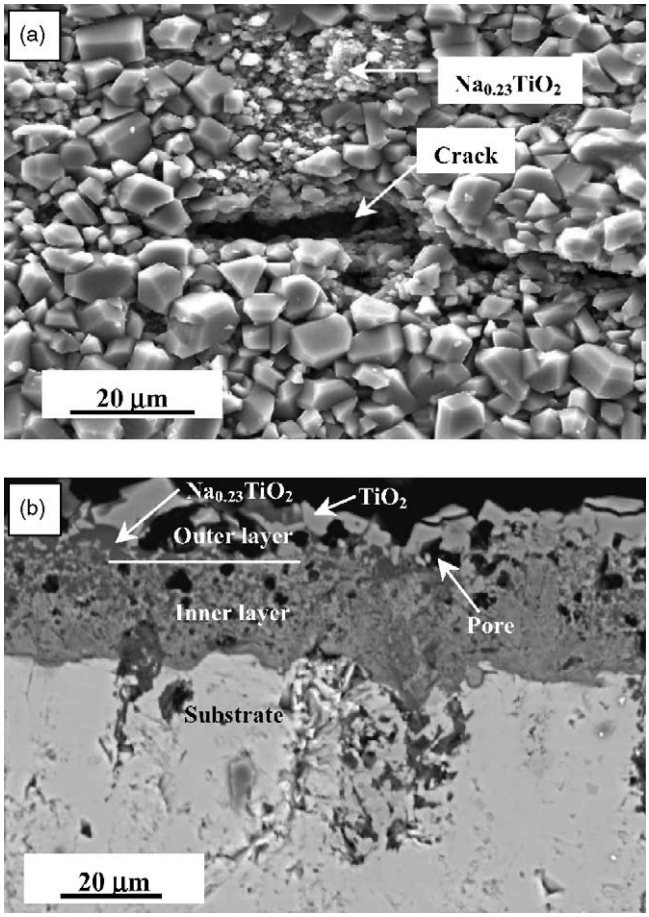

Fig. 6. Morphologies of (a) surface and (b) cross-section of specimen corroded in 25 wt.% Na_2SO_4–75 wt.% NaCl at 850 °C for 100 h.

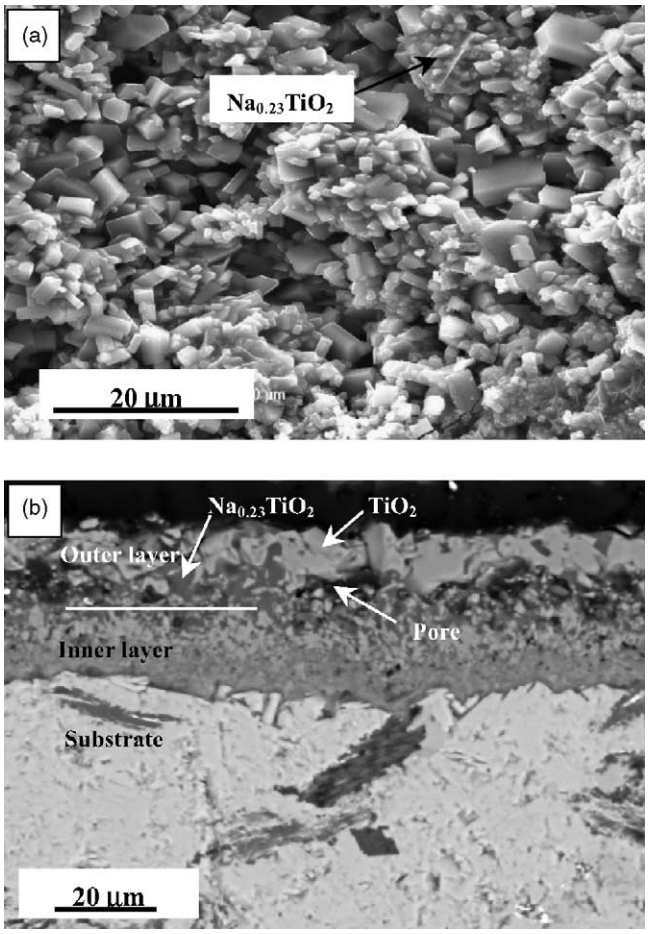

Fig. 7. Morphologies of (a) surface and (b) cross-section of specimen corroded in pure NaCl melt at 850 °C for 100 h.

The microstructures were very similar to those in Fig. 6a and b. However, no crack was observed on the surface of the corrosion layer; less pores existed in the cross-section, which denoted that the specimen exhibited better hot corrosion resistance in pure NaCl melt. The phase compositions were also determined to be TiO_2 and $Na_{0.23}TiO_2$ by XRD (see Fig. 5).

3.3. Mechanism for the corrosion of Ti_3SiC_2

It is reported that Ti_3SiC_2 suffered severe hot corrosion in the eutectic K_2CO_3 and Li_2CO_3 mixture at 850 °C.[9,10] It was considered that corrosion of this material in the eutectic K_2CO_3–Li_2CO_3 mixture was caused by the dissolution of SiO_2 and TiO_2, which formed by the oxidation of Ti_3SiC_2 owing to dissolved oxygen.[7]

$$Ti_3SiC_2 + 5O_2 \rightarrow 3TiO_2 + SiO_2 + 2CO \quad (1)$$

The corrosion rate was related to the basicity of carbonates. However, Na_2SO_4 tended to dissociate less than (Li,K)-carbonates and hence is more acidic. Shi and Rapp[14] measured the solubility of SiO_2 in Na_2SO_4 for a_{Na_2O} from 10^{-11} to 10^{-14} at 900 °C. Over the range they obtained a very limited and constant solubility of 3.2 ± 1.8 ppm by weight. However, this experimental results revealed that when the concentration of Na_2SO_4 was higher than 35 wt.%, the corrosion rate of Ti_3SiC_2 in molten Na_2SO_4–NaCl salts at 850 °C was very fast (the average mass loss rate was about 8.75 mg cm^{-2} h^{-1} in 8 h), which was higher than that of Ti_3SiC_2 corroded in the mixture of $(Li,K)_2CO_3$ melts at 850 °C (the average mass loss rate was about 3.75 mg cm^{-2} h^{-1} in 8 h).[10] The reason for this was thought to be related to C existing in Ti_3SiC_2. C and CO could act as a reducing agent at high-temperature. It is reported that the addition of carbon to pure sodium sulfate led to the formation of CO_2 or CO, which made the following process favorable:[15]

$$Na_2SO_4(l) + 2C(s) \rightarrow Na_2S + 2CO_2(g) \quad (2)$$

$$Na_2SO_4(l) + 4C(s) \rightarrow Na_2S + 4CO(g) \quad (3)$$

The formation of Na_2S has been observed experimentally in a pure Na_2SO_4 + C system.[15] According to the above reactions, we could conclude that the released CO from the oxidation of Ti_3SiC_2 might be sufficient to create basic con-

ditions:

$$Na_2SO_4(l) + 4CO(s) \rightarrow Na_2S + 4CO_2(g) \quad (4)$$

$$Na_2S + Na_2SO_4 \rightarrow 2Na_2O + SO_2 + S \quad (5)$$

Na_2SO_4 and Na_2S could form a eutectic melts with a melting temperature of about 740 °C and react with the newly formed SiO_2 and TiO_2 according to the following reactions:[16]

$$Na_2SO_4(l) + Na_2S + xSiO_2(s) \rightarrow 2Na_2O^{\bullet}xSiO_2(l) + SO_3(g) + S(l) \quad (6)$$

$$Na_2SO_4(l) + Na_2S + yTiO_2(s) \rightarrow 2Na_2O^{\bullet}yTiO_2(l) + SO_3(g) + S(l) \quad (7)$$

where x and y were variatable coefficients. Therefore, when the concentration of Na_2SO_4 was higher than 35 wt.%, the corrosion rate of Ti_3SiC_2 in Na_2SO_4–NaCl melts was very high. On the other hand, because the melting point of NaCl (801 °C) was lower than that of Na_2SO_4 (884 °C), the mixed salts melted and liquid corrodent covered the samples at 850 °C, which would lead to faster corrosion rate. According to reactions (6) and (7), when Na_2SO_4 and Na_2S penetrated the out layer and corrosion occurred at the interface of corrosion layer and substrate, sulfur would segregated in the inner layer. This was the reason why sulfur was detected in the inner corrosion layer. Sulfur segregated in the inner layer resulted in corrosion products spall off easily, corrosion products could not protect substrate, and then corrosion of sample was accelerated.

It is reported that some alloys such as Ti–50Al, Ti–50Al–10Cr exhibited good hot corrosion resistance in Na_2SO_4 melt at 900 °C, however, these alloys suffered severe hot corrosion attack in Na_2SO_4–NaCl melts at 850 °C.[17] As mentioned previously, Ti_3SiC_2 exhibited excellent corrosion resistance in pure NaCl melt. The main reason might be related to stable protective oxide film formed on the specimen surface in NaCl melt. During the initial corrosion stage, Ti_3SiC_2 was oxidized by the dissolved oxygen in the NaCl melt according to reaction (1). Oxygen diffused through the molten salts to specimens and reacted with NaCl and newly formed TiO_2 and SiO_2. Some investigators proposed reactions as follows:[18,19]

$$2NaCl(g) + 0.5O_2(g) + 2SiO_2(s) \rightarrow Na_2Si_2O_5(l) + Cl_2(g) \quad (\Delta G^{\circ} = 113.7\,kJ\,mol^{-1}\ at\ 1200\,K) \quad (8)$$

$$2NaCl(g) + 0.5O_2(g) + TiO_2(s) \rightarrow Na_2Ti_2O_3(l) + Cl_2(g) \quad (\Delta G^{\circ} = 142.3\,kJ\,mol^{-1}\ at\ 1200\,K) \quad (9)$$

However, both reactions (8) and (9) are not thermodynamically favored. Considering most oxygen dissolved in melts was consumed by reaction (1) and resulted in very low oxygen partial pressure in the melts, which was also adverse to reactions (8) and (9). Therefore, Ti_3SiC_2 exhibited excellent corrosion resistance in the molten NaCl.

As mentioned in the above sections, before hot corrosion occurred, Ti_3SiC_2 was oxidized first to form TiO_2 and SiO_2. SiO_2 played a crucial role for oxidation resistance. The reaction process could be modeled with rate control by an interfacial solution of SiO_2 and TiO_2 into the melts at a rate proportional to the instantaneous melt composition.[20] When the specimens corroded in the mixture of 25 wt.% Na_2SO_4 + 75 wt.% NaCl melts, the mixture of melts could not create sufficient basicity (a_{Na_2O}). The oxidation rate of Ti_3SiC_2 was higher than the reaction rate of oxides (TiO_2 and SiO_2) with the mixture of melts. Therefore, the protective mixture of oxide layer (SiO_2 + TiO_2) formed on the specimen surface. Actually, the mixed oxide layer was observed in Figs. 6b and 7b. Once the protective oxide layer formed on the substrate, the hot corrosion rate of specimens would decrease dramatically. This was the main reason why corrosion rate was very slow in the mixture of 25 wt.% Na_2SO_4 + 75 wt.% NaCl melts.

As described above, many pores existed in each cross-sections of corrosion layer. According to reactions (1)–(5), CO, CO_2, and SO_2 would generate during oxidation and hot corrosion. These gases diffused outward from substrate through melts. Parts of bubbles released from the molten salts, however, parts of bubbles trapped in the final corrosion product, thus the pores in the corrosion layer formed. Similar phenomenon was observed when α-SiC was corroded at 1000 °C by Na_2SO_4.[15]

4. Conclusions

Ti_3SiC_2 suffered severe hot corrosion attack in the mixture of Na_2SO_4–NaCl melts when the concentration of Na_2SO_4 was higher than 35 wt.% at 850 °C. The corrosion layer had duplex microstructure; some radial and transverse cracks existed in the outer and inner layer, respectively. The corrosion products tended to spall from substrate. C and CO acted as reducing agents at high-temperature and increased the basicity of melts greatly and resulted in high corrosion rate. The presence of NaCl accelerated the corrosion rate for its lower melting point in the mixture of Na_2SO_4–NaCl melts. When the concentration of Na_2SO_4 was lower than 25 wt.% corrosion rate of Ti_3SiC_2 was quite slow and the corrosion products did not spall at 850 °C. Because of low basicity in the mixture of melts, the protective oxide layer of TiO_2 + SiO_2 formed and led to low corrosion rate of Ti_3SiC_2.

Acknowledgements

This work was sponsored by National Outstanding Young Scientist Foundation of China for Y.C. Zhou under Grant No. 59925208 and Natural Science Foundation of China (Nos. 50172050 and No. 50232040).

References

1. Barsoum, M. W. and El-Raghy, T., Synthesis and characterization of a remarkable ceramic: Ti_3SiC_2. *J. Am. Ceram. Soc.* 1996, **79**(7), 1953–1956.
2. Sun, Z. M. and Zhou, Y. C., Synthesis of Ti_3SiC_2 powders by a solid–liquid method. *Scripta Mater.* 1999, **41**(1), 61–66.
3. Tong, X., Yano, T. and Iseki, T., Synthesis and mechanical properties of Ti_3SiC_2/SiC composites. *J. Mater. Sci.* 1995, **30**, 3087–3090.
4. Zhou, Y. C. and Sun, Z. M., Microstructure and mechanism of damage tolerance for Ti_3SiC_2 bulk ceramics. *Mater. Res. Innovat.* 1999, **2**(6), 360–363.
5. Arunajatesan, S. and Carim, A. H., Synthesis of titanium silicon carbon. *J. Am. Ceram. Soc.* 1995, **78**, 667–672.
6. Zhou, Y. C. and Sun, Z. M., Micro-scale deformation of polycrystalline Ti_3SiC_2 under room temperature compression. *J. Eur. Ceram. Soc.* 2001, **21**(8), 1007–1010.
7. Sun, Z. M., Zhou, Y. C. and Li, M. S., Oxidation behavior of Ti_3SiC_2-based ceramic at 900–1300 °C in air. *Corrs. Sci.* 2001, **43**, 1095–1109.
8. Kofstad, P., *High Temperature Corrosion*. Elsevier Applied Science, London and NewYork, 1988, pp. 465.
9. Liu, G. M., Li, M. S. and Zhou, Y. C., Corrosion behavior of Ti_3SiC_2 and siliconized Ti_3SiC_2 in the mixture of K_2CO_3 and Li_2CO_3 melts at 750 °C. *J. Mater. Sci. Lett.* 2002, **21**(22), 1755–1757.
10. Liu, G. M., Li, M. S. and Zhou, Y. C., Corrosion behavior and strength degradation of Ti_3SiC_2 in the eutectic K_2CO_3 and Li_2CO_3 mixture. *J. Eur. Ceram. Soc.* 2003, **23**(11), 1957–1962.
11. Liu, G. M., Li, M. S. and Zhou, Y. C., Hot corrosion of Ti_3SiC_2-based ceramic superficially deposited with Na_2SO_4 at 900 °C and 1000 °C in air. *Corrs. Sci.* 2002, **45**(6), 1217–1226.
12. Zhou, Y. C., Sun, Z. M., Chen, S. Q. and Zhang, Y., In-situ hot pressing/solid liquid reaction synthesis of dense Ti_3SiC_2 bulk ceramics. *Mater. Res. Innovat.* 1998, **2**(3), 142–146.
13. Jacobson, N. S., Kinetics and mechanism of corrosion of SiC by molten salts. *J. Am. Ceram. Soc.* 1986, **69**(1), 74–82.
14. Shi, D. Z. and Rapp, R. A., The solubility of SiO_2 in fused Na_2SO_4 at 900 °C. *J. Electrochem. Soc.* 1986, **133**(4), 849.
15. Jacobson, N. S. and Smialek, J. L., Hot corrosion of sintered α-SiC at 1000 °C. *J. Am. Ceram. Soc.* 1985, **68**(8), 432–439.
16. Berthold, C. and Nickel, K. G., Corrosion of Si-based non-oxide ceramics by molten Na_2SO_4. *Key Eng. Mater.* 1997, **132–136**, 1588.
17. Tang, Z. L., Wang, F. H. and Wu, W. T., Hot-corrosion behavior of TiAl-base intermetallics in molten salts. *Oxid. Met.* 1999, **51**, 235–250.
18. Hara, M. and Kitagawa, Y., Effect of trace amount of NaCl vapor on high-temperature oxidation of TiAl. *Oxid. Met.* 1999, **52**, 77–94.
19. Jacobson, N. S., Sodium sulfate: deposition and dissolution of silica. *Oxid. Met.* 1989, **31**, 91–103.
20. Riley, F. L., The corrosion of ceramics: where do we go from here. *Key Eng. Mater.* 1996, **113**, 1–14.